Published in Proceedings of the 2004 ASME Wind Energy Symposium, Paper No. AIAA-2004-1002, pp. 424-434, Reno, Nevada, January 2004.

AIAA-2004-1002

ON ESTIMATION OF COHERENCE IN INFLOW TURBULENCE BASED ON FIELD MEASUREMENTS*

Korn Saranyasoontorn[1]
Lance Manuel[1]
Paul S. Veers[2]
[1]Department of Civil Engineering, University of Texas at Austin, Austin, TX 78712
[2]Wind Energy Technology Department, Sandia National Laboratories, Albuquerque, NM 87185

ABSTRACT

The Long-Term Inflow and Structural Test (LIST) program, managed by Sandia National Laboratories, is gathering inflow and structural response data on a modified version of the Micon 65/13 wind turbine at a site near Bushland, Texas. With the objective of establishing correlations between structural response and inflow, previous studies have employed regression and other dependency analyses to attempt to relate loads to various inflow parameters. With these inflow parameters that may thought of as single-point-in-space statistics that ignore the spatial nature of the inflow, no significant correlation was identified between load levels and any single inflow parameter or even any set of such parameters, beyond the mean and standard deviation of the hub-height horizontal wind speed. Accordingly, here, we examine spatial statistics in the measured inflow of the LIST turbine by estimating the coherence for the three turbulence components (along-wind, across-wind, and vertical). We examine coherence spectra for both lateral and vertical separations and use the available ten-minute time series of the three components at several locations. The data obtained from spatial arrays on three main towers located upwind from the test turbine as well as on two additional towers on either side of the main towers consist of 291 ten-minute records. Details regarding estimation of the coherence functions from limited data are discussed. Comparisons with standard coherence models available in the literature and provided in the IEC guidelines are also discussed.

INTRODUCTION

The present study was motivated by failure to find meaningful correlation between turbine loads (extremes and fatigue) and simple inflow parameters that did not describe the spatial structure of the inflow. For example, in previous regression studies by Nelson *et al.* (2003) it was found that single-point-in-space statistics of inflow (e.g., at the hub height) were insufficient for predicting wind turbine loads such as extreme edgewise (in-plane) or flapwise (out-of-plane) bending moments at the blade root. It was, thus, thought to be useful to study the full spatial description of the random inflow turbulence field. The availability of inflow data (as time series segments) at multiple locations through the Long-Term Inflow and Structural Test (LIST) program offers a unique opportunity to estimate the spatial statistics of the inflow. It is our belief that future studies on the correlation of wind turbine loads to inflow may be improved if such spatial statistics are taken into consideration.

One means of identifying the frequency-dependent and random nature of interactions in the inflow at different locations and how these might influence turbine loads is to study the coherence of along-wind (u), across-wind (v), and vertical (w) turbulence components. For design purposes, prescribed models for each turbulence component, including power spectra and coherence spectra, are required in order to perform simulations of the complete inflow field. Computational aerodynamic analysis software uses this simulated inflow to compute the structural response that may be used to determine design loads. Different theoretical turbulence models utilized to construct full-field wind simulation may result in significant differences in design extreme or fatigue loads for wind turbines. Veldkamp (2003) compared prediction of turbine tower and blade fatigue loads based on inflow simulation with several models. For example, with two of the models studied – the Mann uniform shear model (Mann, 1994) where the spectral tensor for atmospheric surface layer turbulence in neutral conditions based on the Navier-Stokes equations as well as conservation of mass is modeled; and the Veers model (Veers, 1988) where the three turbulence components are assumed independent – he concluded that predicted fatigue design loads were quite different. This finding suggests the importance of selecting appropriate turbulence models in design. We are also therefore interested in assessing the validity of the existing turbulence models currently defined in the

IEC standard (IEC/TC88 61400-1, 1998) by comparing them with coherence spectra of full-field wind turbulence components estimated directly from field measurements from the LIST program managed by Sandia National Laboratories.

Another motivation for the present study is that although several field studies of the coherence structure of turbulence have been carried out in Europe (see, for example, Mann *et al.*, 1991; Schlez and Infield, 1998; Larsen and Hansen, 2003), comparatively far fewer such studies (especially with the appropriate heights and separation distances that are useful for wind turbine applications) have been carried out in the United States where the environmental conditions and coherence structure of the inflow may be different.

Recent findings from inflow measurements carried out in Denmark by Larsen and Hansen (2003) reveal that when plotted against the non-dimensional, reduced frequency, f_r equal to fD/U (where f is the frequency, D is the separation distance and U is the mean horizontal wind velocity), the coherence function of the along-wind (u) turbulence component decays faster with vertical separation than it does for the same separation laterally. However, these conclusions are based upon limited data and the lateral separation distances in that study were greater than 79 meters (much larger than the separations that we will study for the LIST turbine). Also, in that study, only the along-wind coherence (i.e., *uu*-coherence) was considered. Here, the available inflow data from the LIST program allow us to analyze the coherence function of all three turbulence components at different vertical and lateral separations. In addition, we also study the cross-coherence of each pair of distinct turbulence components at the center of the rotor circle.

In the following, power spectra and coherence spectra for the three turbulence components are estimated using several of the LIST data sets by employing the Welch's modified Periodogram (block-averaging) spectral estimation method. To facilitate understanding of the coherence as a function of primary inflow parameters, we study these separately for different bins defined on the basis of hub-height mean and standard deviation values of horizontal wind speed. Since only limited data from the first phase of the LIST program were used and the estimations of the coherence functions may be subject to large statistical uncertainty, error statistics of the estimated spectra defined in terms of bias, variance, and confidence limits are discussed.

THE LIST DATA SET

The data sets employed to estimate spatial coherence spectra throughout this study were provided by Sandia National Laboratories through the ongoing Long-Term Inflow and Structural Test (LIST) program (Sutherland *et al.*, 2001). The LIST program has made available continuous time series of atmospheric inflow conditions as well as structural response data for a modified Micon 65/13 wind turbine (referred to as the LIST turbine in this study). This measurement campaign is taking place at the USDA-ARS site in Bushland, Texas which is characteristic of a Great Plains site with essentially flat terrain and the primary wind direction at the site is from 215^o with respect to True North (see Fig. 1 for details of the LIST test site).

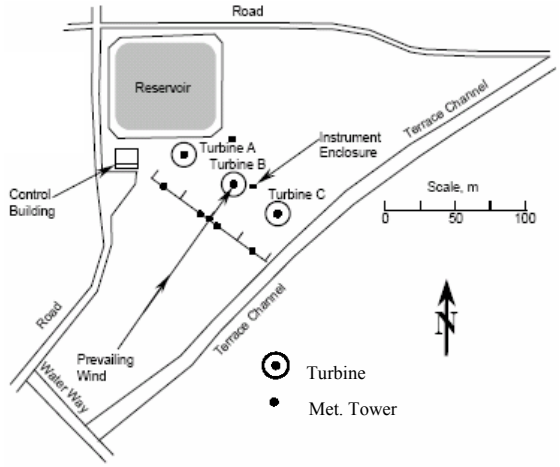

Figure 1: Schematic view of the LIST Test site showing the LIST turbine (Turbine B) and five meteorological towers (taken from Jones *et al.*, 2001).

The data were recorded as ten-minute segments, each of which contains approximately 18,000 data points, at a sampling rate of 30 Hz (implying a Nyquist frequency of 15 Hz). Characterization of the inflow in this study relies on an array of five sonic anemometers mounted on three meteorological towers located approximately 30 meters in front of the LIST turbine as shown in Fig. 1. The center tower is directly upwind of the LIST turbine. The other two towers are one rotor-disk radius to the left and right of the center tower. The five sonic anemometers are mounted as follows: at hub height which is 23 meters from the ground; at the top and bottom of the rotor circle; and at positions left and right of the center of the rotor circle (see Fig. 2). Two additional meteorological towers located in front of the sister turbines, approximately 38 meters away from the center tower on the left and right, were constructed to measure horizontal wind velocities at the hub height

using cup anemometers. The additional inflow data from these two towers are used to study the coherence of the along-wind turbulence component with this greater lateral separation.

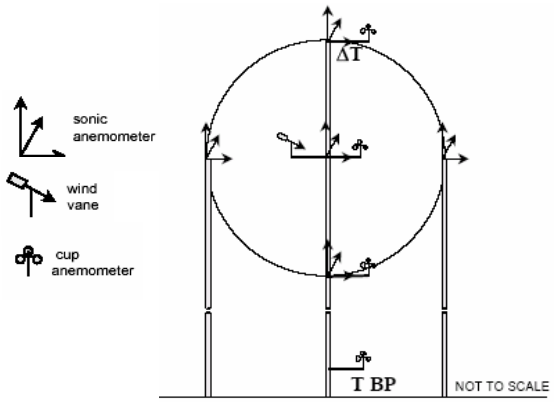

Figure 2: Primary inflow instrumentation on the main meteorological towers upwind of the LIST turbine (taken from Jones *et al*., 2001).

In preparation for the analysis, 291 of the available ten-minute data records were grouped into bins, depending on the horizontal mean wind velocity at hub height, U_{hub}, and the standard deviation of the same hub-height velocity, σ_{hub}. This was done in order to obtain a representative sample of data sets for each bin so that conclusions could be made about the dependence of coherence on these inflow parameters, regarded as primary by the wind energy community. The number of available data sets for each bin is shown in Table 1.

σ_{hub} (m/s)	U_{hub} (m/s)					
	7-9	9-11	11-13	13-15	15.17	>17
0.5-1.0	52	29	0	0	0	0
1.0-1.5	22	**33**	20	3	0	0
1.5-2.0	5	21	**25**	8	5	3
2.0-2.5	3	6	6	14	**14**	9
2.5-3.0	0	2	0	2	2	7

Table 1: The number of ten-minute data sets in each bin characterized by the mean, U_{hub}, and standard deviation, σ_{hub}, of the hub-height horizontal wind velocity.

All the bins that contained a sufficient number of samples were analyzed; however, only results based on data sets from three bins are discussed in the following. These selected bins correspond to the boldfaced entries in Table 1. For simplicity, these are referred to as Bins A, B, and C in the following. The range in values of the mean, U_{hub}, and the standard deviation, σ_{hub}, of the horizontal wind speed at hub height for each of the three bins is shown in Table 2 along with the number of data sets available, N_g, and the average integral length scale, L, for each bin.

Bin	U_{hub} (m/s)	σ_{hub} (m/s)	N_g	L (m)
A	9-11	1.0-1.5	33	69
B	11-13	1.5-2.0	25	98
C	15-17	2.0-2.5	14	141

Table 2: Three bin classes used in this numerical studies and their number of ten-minute data sets, N_g, and average integral length scale, L.

COHERENCE ESTIMATION: A REVIEW

A mathematical expression of the (magnitude-squared) coherence function, $\gamma^2(f)$, of two stationary random processes, p and q, may be given as:

$$\gamma^2(f) = \frac{|S_{pq}(f)|^2}{S_{pp}(f)S_{qq}(f)} \tag{1}$$

where $S_{pp}(f)$ and $S_{qq}(f)$ are the one-sided (auto-)power spectral density functions of p and q, respectively, at frequency, f; and $S_{pq}(f)$ is the one-sided complex-valued cross-power spectral density function between the two processes. Note that the coherence, $\gamma^2(f)$, is always greater than or equal to zero and by Schwarz's inequality, it always less than or equal to unity. For a finite-length data record, the coherence can be estimated from ensemble estimates of the auto- and cross- spectra; namely,

$$\hat{\gamma}^2(f) = \frac{|\hat{S}_{pq}(f)|^2}{\hat{S}_{pp}(f)\hat{S}_{qq}(f)} \tag{2}$$

where the quantities with a caret indicate that each is estimated from the limited data (N_g data sets for each bin). Because of the use of limited data and of records of finite length, the estimates in Eq. (2) have unavoidable statistical errors. For example, an obvious distortion will occur if one tries to compute the coherence function by using only one realization each of the two processes, p and q. For such an estimation procedure, the computed coherence function will be identically equal to unity at all frequencies. In practice, each sampled time series is therefore split into N sub-segments to prevent this source of distortion. For N non-overlapping realizations of a stationary, Gaussian random process, the bias, *Bias*, and the variance, *Var*, of the coherence spectrum estimate at any frequency due to time-record truncation effects were derived (Carter, 1972) and may be expressed as:

$$Bias(\hat{\gamma}^2) \approx \frac{1}{N} - \frac{2}{N+1}\gamma^2 + \frac{1!(N-1)}{\Pi_{i=1}^{2}(N+i)}\gamma^4 + \frac{2!(N-1)}{\Pi_{i=1}^{3}(N+i)}\gamma^6 \approx \frac{1}{N}\left(1-\gamma^2\right)^2 \quad \text{for large } N \tag{3}$$

$$Var(\hat{\gamma}^2) \approx \frac{1-N}{N(N+1)}\left\{\begin{array}{l} \frac{1}{N} + 2\gamma^2\frac{N-2}{N+2} \\ -2\gamma^4\frac{N(2N^2-N-2)+3}{\Pi_{i=1}^{3}(N+i)} \\ +2\gamma^6\frac{N(N^3-6N^2-N+10)-8}{\Pi_{i=1}^{4}(N+i)} \end{array}\right\} \approx \frac{2}{N}\gamma^2(1-\gamma^2)^2 \quad \text{for large } N \tag{4}$$

It is recognized that allowing for overlapping of sub-segments can further reduce the statistical variability of the estimates because of the greater number of degrees of freedom used. Experimental investigation by Carter (1972) where a Hanning data window was utilized suggests that fifty-percent overlapping is an optimal choice as a compromise between reduction in standard error and computation time.

Besides conventional bias as predicted by Eq. (3), bias power leakage effects may be introduced if the selected resolution bandwidth is wide relative to the actual range of frequencies associated with a peak in the spectrum. This category of bias, which is known as "resolution bias" may lead to large distortions near the peak of the spectrum. In studying turbulence components, this type of bias may be present due to the significant amount of energy at low frequencies. Even though a theoretical expression of this bias is not available, Jacobsen (1993) concluded from numerical simulation studies that resolution bias effects will occur especially when the number of degree of freedom increases. This is typically associated with the number of (overlapping) sub-segments used and when the coherence values are close to unity. Thus, under certain circumstances, this resolution bias may dominate the conventional bias (Eq. (3)) resulting from a finite number of statistical realizations. Jacobsen (1993) did not report any systematic variance dependency on power leakage from his experiments, indicating that the variance (or standard error) in coherence spectra may be estimated by Eq. (4) alone.

Another source of bias in estimating coherence is due to possible time delay between the two signals, *p* and *q*, that can be easily detected either by simply observing the corresponding cross-covariance function of the two time series or by observing a linear trend in the phase spectrum. This source of bias might be important when studying coherence in turbulence components over large lateral separations.

ESTIMATION PROCEDURE

For each bin defined in Table 2, the wind velocities in the measured frame of reference are transformed into the standard micrometeorological coordinate system, defined as along-wind (*u*), across-wind (*v*), and vertical (*w*) components. Each ten-minute time series is transformed into a zero-mean process that is detrended (this yields the signal, x_t). Then, a high-pass filter, is applied in order to reduce possible bias caused by leakage effects (see Jenkins and Watts, 1968) yielding the filtered signal, $y_t = 1.01x_t - 1.00x_{t-1}$. Next, the ten-minute time series of interest are partitioned into a suitable number of fifty-percent overlapped sub-segments, N_d, each of which is considered as a realization of the process for use in estimation of the spectra. Hence, each bin class yields a total of $N=N_d \times N_g$ realizations, each of which is multiplied by a Hanning data window, before raw power and cross spectra using the Fast Fourier Transform (FFT) algorithm are finally computed. Next, these spectra derived from the realizations are averaged in each bin to obtain representative power spectral density functions and cross-power spectral density functions for use in Eq. (2) to compute the coherence spectrum, $\hat{\gamma}^2(f)$. This coherence estimate is then bias-corrected using Eq. (3).

NUMERICAL STUDIES

Several issues related to coherence estimates based on the LIST field measurements are investigated. For simplicity, we will refer to power spectral density function of the along-wind (*u*), across-wind (*v*), and vertical (*w*) turbulence components as *u*-, *v*-, and *w*-power spectra, respectively. Similarly, for lateral and vertical separations studied, we refer to coherence functions of the along-wind, across-wind, and vertical turbulence components as *uu*-, *vv*-, and *ww*-coherences, respectively. Finally, we study cross-coherence between any two turbulence components at the center of the rotor circle and refer to these as *uv*-, *uw*-, and *vw*- coherences.

Choices of Sub-segment length

To achieve good estimates of coherence spectra, it is necessary to use an appropriate number of overlapping sub-segments that can provide satisfactorily small amounts of bias and standard error, without introducing much spectral distortion. A large number of sub-segments, which is associated with small individual sub-segment length, might limit confidence intervals on the coherence estimate but it might introduce unacceptable spectral distortion and, thus, lose the fine structure

of the coherence especially near the low frequency region where the coherence value is large, approaching unity. A rational approach was adopted in this study whereby bias-corrected (magnitude-squared) coherence spectra were estimated for different numbers of sub-segments for a ten-minute time series. These estimates were then compared until an optimal number of sub-segments was found. For the sake of illustration, we describe how this optimal number of sub-segments was arrived at when estimating the *uu*-coherence for a lateral separation of 15.4 meters. A total of 25 data sets were taken from Bin B (U_{hub} = 11-13 m/s and σ_{hub} = 1.5-2.0 m/s). The same procedure may be applied for other turbulence components and/or for vertical separations. Figure 3(a) shows estimated *uu*-coherence spectra (for 15.4 meters lateral separation) based on 2, 4, 8, 16, and 32 sub-segments in each ten-minute record. Figure 3(b) shows estimates of the coherence spectrum along with 90-perecent confidence intervals with the optimal number of sub-segments, equal to 8 here.

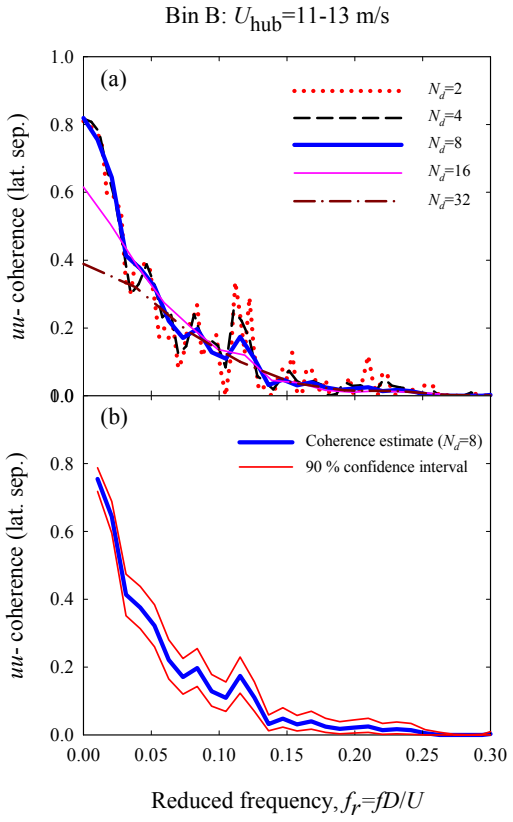

Figure 3: (a) Estimates of *uu*-coherence spectra for a lateral separation distance of 15.4 meters using data from Bin B and different numbers of sub-segments, N_d, (b) Estimate of the *uu*-coherence spectrum and 90-percent confidence intervals using N_d=8.

In this illustration, the number of sub-segments, N_d, that is less than or equal to 8 does not cause severe distortion that can result from sub-segments that are too short. A total of 200 realizations (8×25), is selected for estimating the coherence spectrum since this provides the smallest standard error (compared to lower values of N_d that have similar bias) and still has very slight spectral distortion (compared to higher values of N_d that have systematically larger resolution bias). Using Eqs. (3) and (4), 90-percent confidence intervals were determined on the bias-corrected coherence spectra. These are shown in Fig. 3(b).

In general, for separation distances of 7.7 and 15.4 meters that are used in this study, splitting the ten-minute time series into four to eight fifty-percent overlapped segments will create individual realizations of about 2-4 minutes length making it possible to resolve frequencies as low as 0.004-0.008 Hz with reasonable statistical confidence (and hence, avoid the problem of resolution expected at the low-frequency peak of coherence spectra). In passing, we point out that for fifty-percent overlapping, each realization will have length equal to 10 minutes divided by (N_d+1)/2 and will be able to resolve frequencies as low as (N_d+1)/1200.

Power spectra

Power spectral density functions of the wind turbulence components were determined for the three Bins A, B, and C before using them to estimate coherence spectra. For the sake of brevity, in Fig. 4, we show power spectra only for Bin B for the three turbulence components at the center point of the rotor circle mast. The estimated spectra show that the energy in the along-wind turbulence component is slightly greater than that in the cross-wind component in the low-frequency range and significantly greater than that in the vertical turbulence component. However, the power spectra for all three turbulence components asymptotically have the same slope and magnitude in the inertial subrange (high-frequency range). For the along-wind (u) turbulence component, the estimated power spectrum is compared with the Kaimal spectrum (Kaimal *et al*., 1972) which is recommended by the IEC standard (IEC/TC88 61400-1, 1998) for wind field simulation purposes. A surface roughness length z_0 of 0.5 centimeters is used with the Kaimal model in the comparison (typical values of z_0 for mown grass terrain are about 0.1-1.0 centimeters). Comparison between the theoretical along-wind turbulence power spectrum and the estimated spectrum from field data (at the height of 23 meters) shows that the estimate spectrum agrees reasonably well over all frequencies with the Kaimal spectral model.

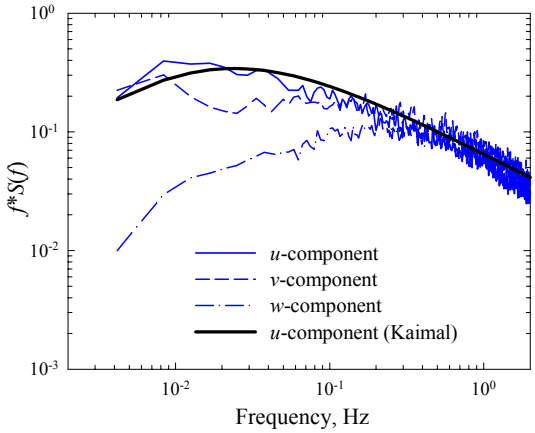

Figure 4: Estimated power spectra of the along-wind (*u*), across-wind (*v*), and vertical (*w*) turbulence components for Bin B and comparison with the Kaimal along-wind turbulence spectrum (assuming a surface roughness of 0.5 centimeters).

Influence of separation distance on coherence

The influence of vertical and lateral separation distances on *uu*-coherence is studied here. The coherence spectra were estimated based on the along-wind (*u*) wind velocity time series at several spatially distributed locations available in Bins A, B, and C with 33, 25, and 14 samples, respectively, as seen in Tables 1 and 2.

For vertical separations of 8.5 and 17.0 meters, the time series used to estimate the spectra were measured by sonic anemometers located at three positions on the center tower mast located approximately 30 meters upwind of the LIST turbine: one at the top of the rotor circle, one at the center (i.e., at the hub height of 23 meters), and one at the bottom of the rotor circle. The *uu*-coherence estimates (for the two vertical separations) along with their 90% confidence intervals are shown in Fig. 5 (top row) for the three different bins. It is observed that, for all bins, and especially for Bins A and B where there was a relatively large number of data sets available (and thus smaller statistical uncertainty), the *uu*-coherence even when plotted against the reduced frequency f_r (equal to fD/U) decreases as vertical separation increases from 8.5 to 17.0 meters. This observation appears to contradict Davenport's exponential coherence model (Davenport, 1961) where the *uu*-coherence spectrum when expressed in terms of the reduced frequency is independent of separation.

For lateral separations of 7.7, 15.4, and 38.2 meters, the time series used to estimate coherence spectra of the along-wind turbulence component were measured by three sonic anemometers located at the three main towers and a cup anemometer on the far right tower (see Fig. 1). All of these anemometers are at the hub height level (23 meters). The *uu*-coherence estimates (for the three lateral separations) are shown in Fig. 5 (bottom row) for the three different bins. Again, when plotted against reduced frequency, f_r, the *uu*-coherence systematically decays faster with increased lateral separation.

When comparing the *uu*-coherence spectra in Fig. 5, it is found that over comparable separation distances, the coherence decays faster with reduced frequency vertically than it does laterally.

Estimated versus theoretical model predictions

In the following, decay rates of the *uu*-coherence for different lateral and vertical separations are compared with those recommended in wind turbine design guidelines such as the IEC exponential model and the von Kármán model.

Decay rates

Exponential decay parameters for *uu*-coherence with vertical separations of 8.5 and 17.0 meters and lateral separations of 7.7 and 15.4 meters are estimated using data from Bin B. Since coherence spectra do not necessarily approach unity (Mann *et al*., 1991), especially for large separations, the decay parameter is estimated as part of a two-parameter exponential fit:

$$\gamma^2(f) = ae^{\left(-b\frac{fD}{U}\right)} \tag{3}$$

where a is one of the parameters constrained to be smaller than or equal to unity since the coherence, by definition, cannot be greater than unity at any frequency; while b is the second parameter that is an indicator of the decay rate.

For vertical separations of 8.5 and 17.0 meters, the parameter, a, was 1.00 and 0.99 while the decay parameter, b, was about 18 and 25, respectively. Similarly, for lateral separations of 7.7 and 15.4 meters, the parameter a was 0.97 and 0.89 while the decay parameter, b, was about 16 and 22, respectively. The exponential fits to the *uu*-coherence spectra are shown in Fig. 6. Based on these fits, it is seen that, the estimated decay parameters for coherence spectra with vertical separation are much larger than those recommended for structural design purposes where a suggested value is about $10\times(U_{23}/U_{10}) \approx 11$ (Simiu and Scanlan, 1996), assuming a power law profile with the rate of 1/7 associated with open terrain, and where U_{23} and U_{10} refer to wind speeds at 23 meters and at 10 meters, respectively. However, the estimated decay parameters for coherence spectra with lateral separation are more in line with recommended values of approximately $16\times(U_{23}/U_{10}) \approx 18$.

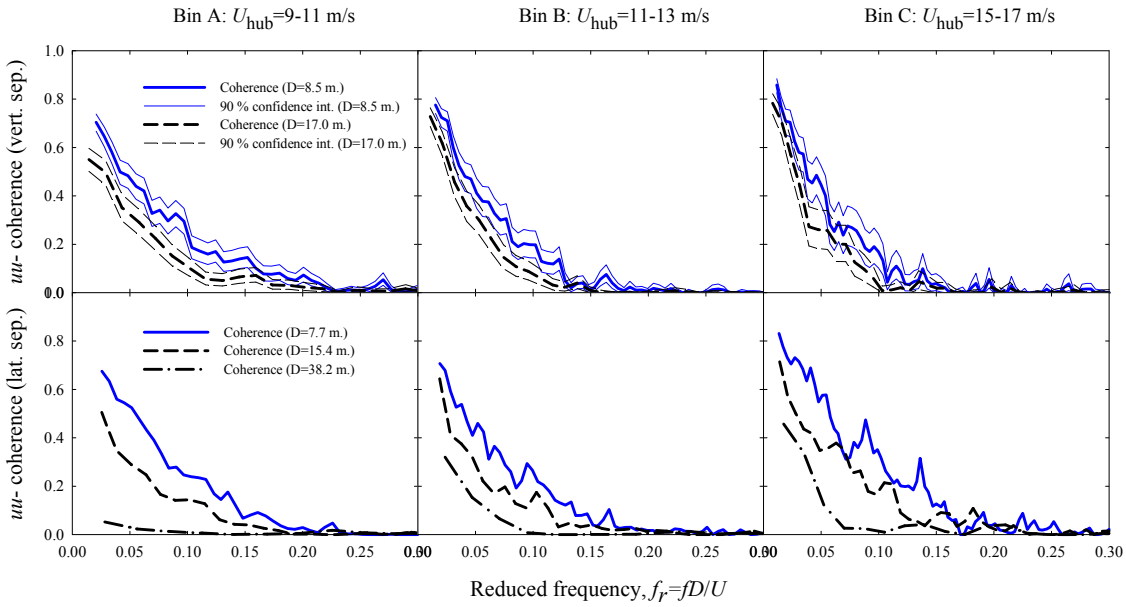

Figure 5: Estimates of *uu*-coherence spectra for vertical separations of 8.5 and 17.0 meters (top row); and for lateral separations of 7.7, 15.4 and 38.2 meters (bottom row) based on data from Bins A, B, and C.

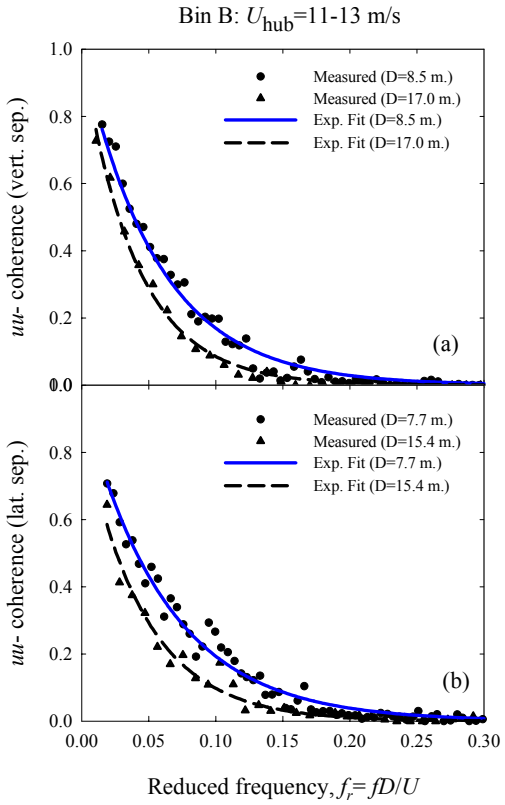

Figure 6: Exponential fits for *uu*-coherence spectra with (a) vertical separations of 8.5 and 17.0 meters and (b) lateral separations of 7.7 and 15.4 meters using data from Bin B.

The IEC Exponential and the von Kármán models

Estimates of *uu*-coherence spectra for Bins A, B, and C for three lateral separations, 7.7, 15.4, and 38.2 meters, are compared with the theoretical von Kármán turbulence spectrum as well as with the modified exponential coherence model recommended in the IEC standard (IEC/TC88 61400-1, 1998). A surface roughness, z_0, of 0.5 centimeters was assumed for use with the von Kármán model, while the integral length scale, L, assumed for use with both models was based on the measured data (see Table 2). In practical situations, the integral length scale may not be available from field measurements and can be instead obtained from the IEC standard (IEC/TC88 61400-1, 1998). It is seen in Fig. 7 that for all bins, the estimated lateral coherence from the LIST field measurements agrees well with the von Kármán model only for the small separation of 7.7 meters (top row of figure). This is probably because assumptions regarding homogeneity and isotropy as well as Taylor's frozen turbulence hypothesis used to derive the von Kármán spectrum are satisfied for small separations. However, at greater separations (here, up to 15.4 and 38.2 meters), the estimated coherence from data is systematically lower than that from either of the two theoretical turbulence models. Comparing the two models, the von Kármán turbulence model predicts lower coherence than the IEC model at all but the lowest frequencies. Neither model predicts the low coherence estimated from data at low frequencies and large separations.

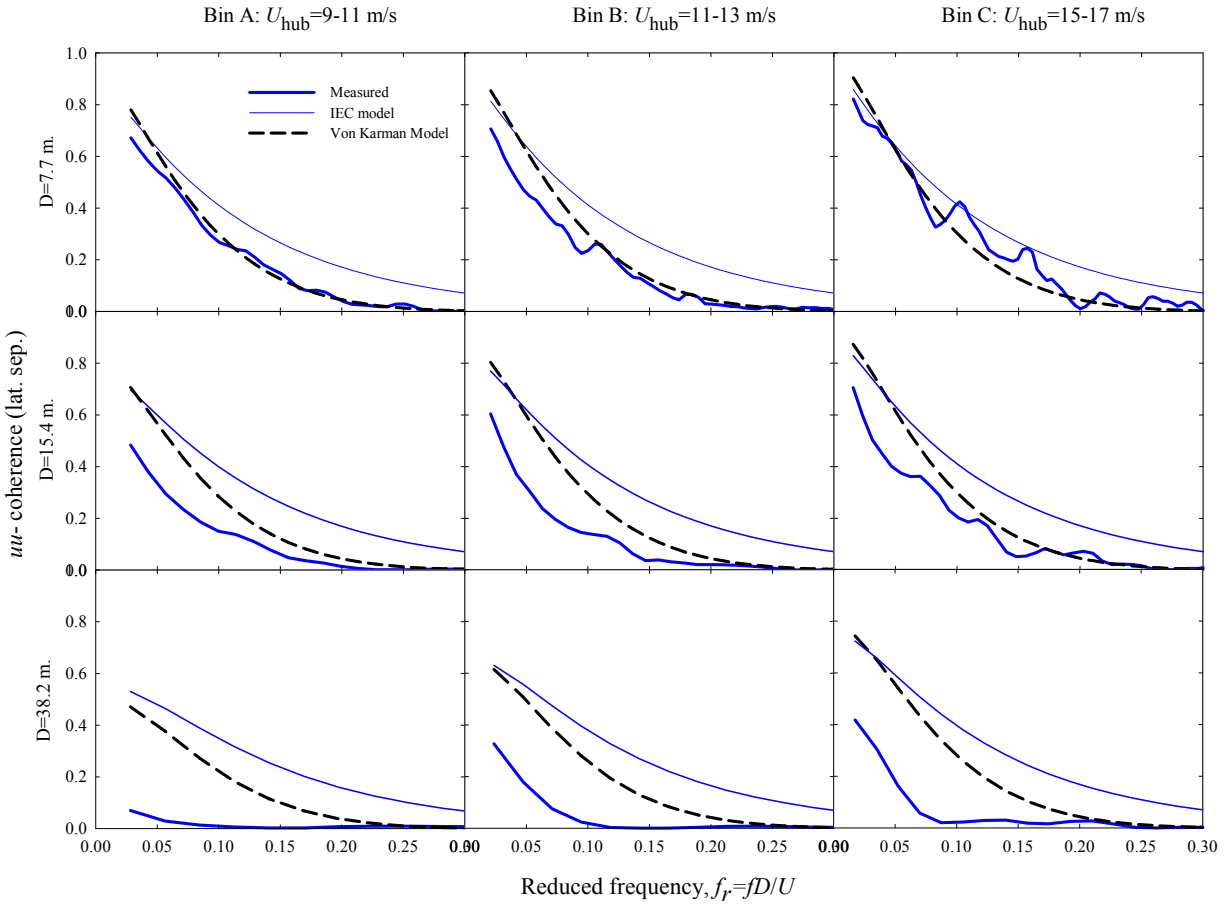

Figure 7: Comparison of the estimated *uu*-coherence spectra for lateral separations of 7.7, 15.4, and 38.2 meters (based on data sets from three bins) with the IEC modified exponential model and the von Kármán models assuming a surface roughness, z_0, of 0.5 centimeters for the von Kármán model and integral length scales as given in Table 2.

Coherence structure of each turbulence component

Thus far, we have only discussed results related to coherence spectra of the along-wind (*u*) turbulence component – i.e., the *uu*-coherence. Coherence spectra for all three turbulence components (i.e., *uu*-, *vv*-, and *ww*-coherences) for two spatial separations are compared here. Figure 8 shows estimated coherence spectra of each turbulence component for lateral separations of 7.7 and 15.4 meters and vertical separations of 8.5 and 17.0 meters based on data in Bins A, B, and C.

For lateral separations, the wind velocity time series used for each component was measured by sonic anemometers mounted at hub-height level of the three center tower masts. It is seen in Fig. 8(a) that the across-wind (*v*) turbulence component is more coherent than the along-wind (*u*) and vertical (*w*) components at both lateral separations, 7.7 and 15.4 meters. Comparing the along-wind and vertical coherence, it is seen for all bins that the *uu*-coherence is larger than the *ww*-coherence in the low frequency range but lower at high frequencies. As expected, coherence in all three turbulence components decreases with increased lateral separation at all frequencies. At the larger lateral separation of 15.4 meters, it is seen that the cross-wind coherence is still the largest of the three components while the along-wind coherence is higher than the vertical coherence over a larger reduced frequency range. These plots in Fig. 8(a) show that the relative coherence levels for the three turbulence components agree with those based on the von Kármán coherence models. However, in Fig. 8(b), this same coherence structure is not observed when studying coherence spectra for different vertical separations. The vertical turbulence component appears to be the most coherent followed by the across-wind and along-wind components. This difference suggests a lack of isotropy that might possibly be explained by vertical instability. For the data sets used, vertical instability as characterized by low Richardson Number values was greatest in Bin A (with lowest wind speeds).

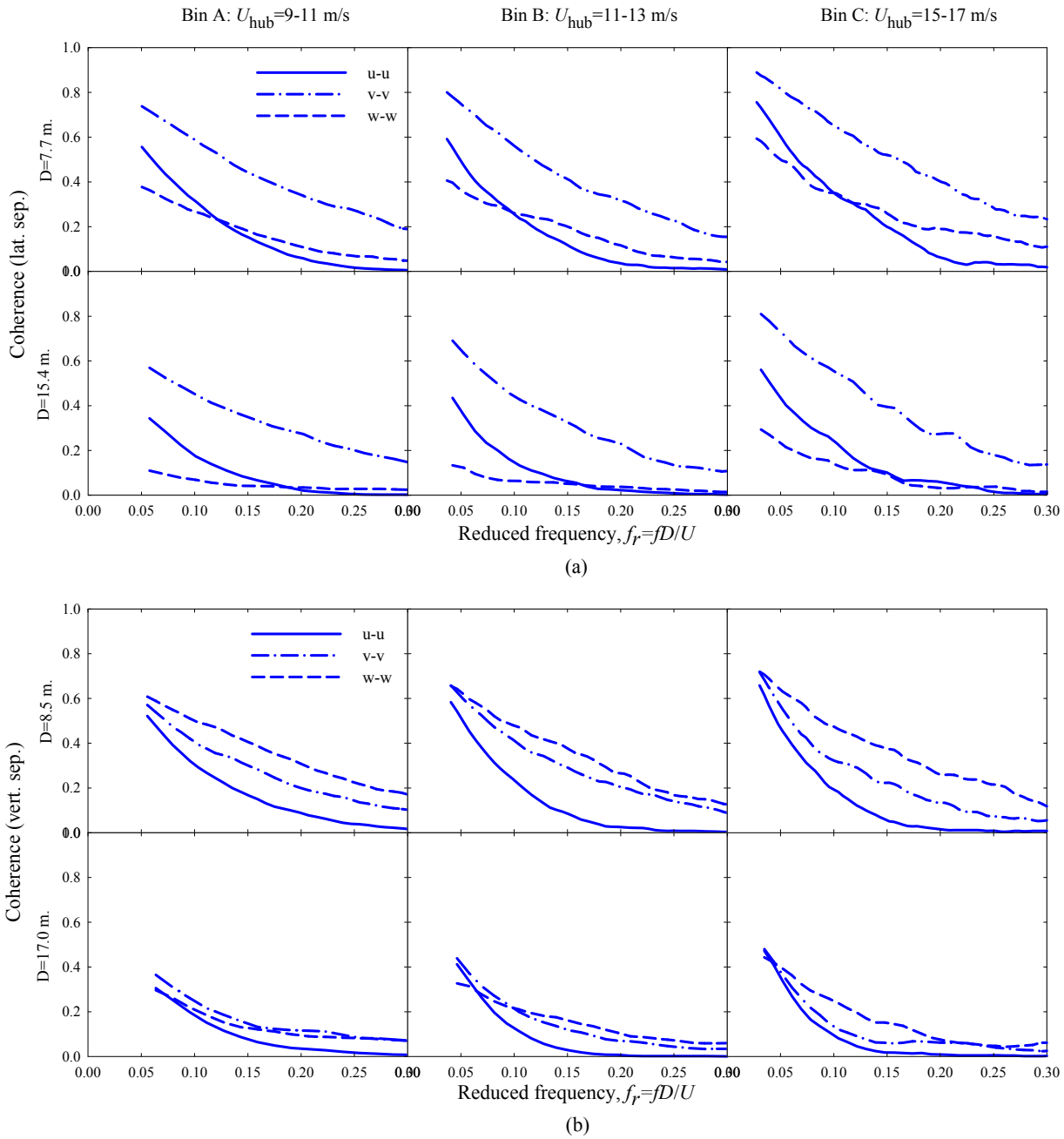

Figure 8: Comparison of estimated coherence spectra for each turbulence component with (a) lateral separations of 7.7 and 15.4 meters and (b) vertical separations of 8.5 and 17.0 meters based on data from Bins A, B, and C.

Cross-coherence

Cross-coherence spectra based on two distinct turbulence components (*u*-*v*, *u*-*w*, and *v*-*w*) recorded at the same point in space (here, the center of the rotor circle with a height of 23 meters) were estimated and the results are summarized in Fig. 9. The figure shows no significant correlation between the along-wind (*u*) and the across-wind (*v*) turbulence components nor between the across-wind (*v*) and vertical (*w*) turbulence components in any of the three bins. This is different from the correlation between the along-wind and vertical components where larger estimates of cross-coherence were observed. This *uw*-coherence may be needed to be modeled when simulating inflow to derive design loads for wind turbines as a recent study by Veldkamp (2003) has also shown that simulated inflow based on a model

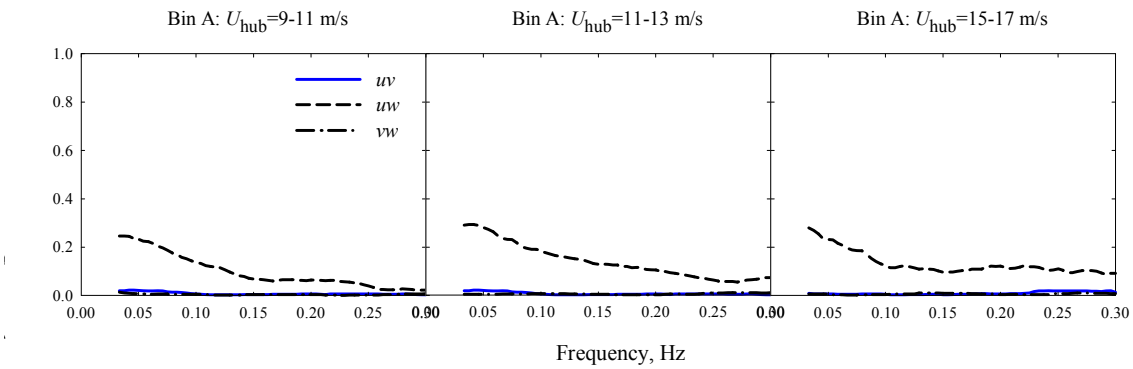

Figure 9: Estimates of cross-coherence spectra at the center of the rotor circle for the turbulence components taken two at a time based on data from Bins A, B, and C.

excluding this correlation may lead to significant differences in fatigue design loads from those derived using a model that includes the cross-coherence between the along-wind and vertical turbulence components.

CONCLUSIONS

In this study, we examined spatial statistics using the LIST program's measured inflow turbulence by obtaining estimates of power and coherence spectra using ten-minute segments of three components of the wind velocity at several different locations. Coherence spectra for different lateral and vertical separations were studied as were cross-coherence spectra between distinct turbulent components. Estimation errors associated with coherence spectra described by bias, variance, and confidence intervals were also discussed. The influence of separation distance on along-wind coherence was studied. Estimated *uu*-coherence spectra based on data were compared with theoretical models. Finally, cross-coherence of different turbulence components was studied. Results obtained for the three different bins defined in Table 2 led to the following general conclusions:

- The along-wind coherence spectra for both vertical and lateral separations, when expressed in terms of reduced frequency, decayed faster with separation distance than is predicted by Davenport's exponential model for which coherence is independent of separation distance.
- Estimated along-wind coherence spectra suggest faster decay with increase in vertical separation than is reported in the literature while for lateral separations, the estimated decay rate agrees fairly well with the literature.
- The von Kármán turbulence model resembles the estimated along-wind coherence spectra better than the IEC modified exponential model but both of them appear to overestimate coherence over large separtions.
- The coherence structure of the along-wind, across-wind, and vertical turbulence components for different lateral separations as estimated based on data was in accordance with the von Kármán model. A very different coherence structure was found when considering vertical separations indicating a lack of isotropy.
- Estimated cross-coherence between the along-wind and across-wind turbulence components as well as between the across-wind and vertical components were far less significant than that between the along-wind and vertical turbulence components.

ACKNOWLEDGEMENTS

The authors gratefully acknowledge the financial support provided by Grant No. 003658-0272-2001 awarded through the Advanced Research Program of the Texas Higher Education Coordinating Board. They also acknowledge additional support from Sandia National Laboratories by way of Grant No. 30914. The authors are grateful to Sandia's Dr. Herbert J. Sutherland for providing us with the field data from the LIST program and they thank him and Dr. William E. Holley for their helpful insights and suggestions.

REFERENCES

1. Carter, G. C., 1972, "Estimation of the Magnitude-Squared Coherence Function," *Naval Undersea Systems Center Report*, No. 4343.
2. Davenport, A. G., 1961, "The Spectrum of Horizontal Gustiness near the Ground in High Winds," *Quart. J. Roy. Met. Soc.*, Vol. 87, pp. 194-211.
3. IEC/TC88 61400-1, 1998, "Wind Turbine Generator Systems Part 1: Safety Requirements," *International Electrotechnical Commission (IEC)*, Ed. 2.
4. Jacobsen, S., 1993, "Statistics of Leakage-Influenced Squared Coherence Estimated by Bartlett's and Welch's Procedures," *IEEE Transactions on Signal Processing*, Vol. 41, No. 1, pp. 267-277.
5. Jenkins G. M. and D. G. Watts, 1968, *Spectral Analysis and its Applications*, Holden-Day Inc., San Francisco, CA.
6. Jones, P. L., H. J. Sutherland, and B. A. Neal, 2001, "LIST/BMI Turbines Instrumentation and Infrastructure," SAND2001-1642, Sandia National Laboratories, Albuquerque, NM.
7. Kaimal, J. C., J. C. Wyngaard, Y. Izumi, and O. R. Cote, 1972, "Spectral Characteristics of Surface Layer Turbulence," *Quart. J. Roy. Met. Soc.*, Vol. 98, pp. 563-598.
8. Larsen, G. C. and K. S. Hansen, 2003, "Spatial Coherence of the Longitudinal Turbulence Component," *EWEC*, Madrid, Spain.
9. Mann, J., L. Kristensen, and M. S. Courtney, 1991, "The Great Belt Coherence Experiment," Risø R-596, Risø National Laboratory, Roskilde, Denmark.
10. Mann, J., 1994, "The Spatial Structure of Neutral Atmospheric Surface-Layer Turbulence," *Journal of Fluid Mechanics*, Vol. 273, pp. 141-168.
11. Nelson, L. D., L. Manuel, H. J. Sutherland, and P. S. Veers, 2003, "Statistical Analysis of Inflow and Structural Response Data from the LIST Program," *Proceedings of the ASME Wind Energy Symposium*, Paper No. AIAA-2003-0867, Reno, Nevada.
12. Simiu, E. and R. H. Scanlan, 1996, *Wind Effects on Structures: Fundamentals and Applications to Design*, 3rd Edition, John Wiley & Sons, Inc.
13. Schlez, W. and D. Infield, 1998, "Horizontal, Two Point Coherence for Separations Greater than the Measurement Height," *Boundary-Layer Meteorology*, Vol. 87, pp. 459-480.
14. Sutherland, H.J., P.L. Jones, and B. Neal, 2001, "The Long-Term Inflow and Structural Test Program," ASME Wind Energy Symposium, AIAA-2001-0039, pp. 1-12.
15. Veers, P. S., 1988 "Three-dimensional Wind Simulation," SAND 88-0512, Sandia National Laboratory, Albuquerque, NM.
16. Veldkamp, D., 2003, "Influence of Wind Field Generation Methods on Wind Turbine Fatigue Loads," *EWEC*, Madrid, Spain.